ISBN: 978-3-95450-191-5 doi:10.18429/JACoW-SRF2017-THYA02

ACHIEVEMENT OF STABLE PULSED OPERATION AT 36 MV/m IN STF-2 CRYOMODULE AT KEK

Y. Yamamoto†, T. Dohmae, M. Egi, K. Hara, T. Honma, E. Kako, Y. Kojima, T. Konomi, T. Kubo, T. Matsumoto, T. Miura, H. Nakai, K. Nakanishi, G. Park, T. Saeki, H. Shimizu, T. Shishido, T. Takenaka, K. Umemori
High Energy Accelerator Research Organization, Tsukuba, Japan

Abstract

In the Superconducting RF Test Facility (STF) in KEK, the cool-down test for the STF-2 cryomdoules with twelve cavities has been done three times since 2014. In 2016, the third cool-down test was successfully done including the capture cryomodule with two cavities, used for Quantum Beam Project in 2012. In this paper, the result of the third cool-down test is presented in detail.

INTRODUCTION

The STF-2 cryomodules are the one and half size cryomodule, defined "Type B" in Technical Design Report (TDR) for International Linear Collider (ILC) [1], with twelve 9-cell STF-type cavities, called CM1 and CM2a, respectively. In the center of CM1, there are one superconducting quadrupole magnet developed by the collaboration between KEK and FNAL [2], and one beam position monitor developed in Accelerator Test Facility (ATF) [3].

The table 1 shows the brief history of STF-2 project. The fabrication of cavities and power couplers started from 2010. In the period of 2013-2014, the cavity string assembly and the cryomodule assembly were done, the STF-2 cryomodules were successfully installed into the STF tunnel, and the investigation for the high pressure gas regulation was done by the local government. In 2014, the first cool-down test was done for the low power measurement by network analyser, the drive test for the slide-jack tuner, and the piezo tuner test by the induced voltage of 500 V [4]. In 2015, the second cool-down test was done for the performance check in the single cavity operation using the 5 MW klystron and the single waveguide system [5, 6]. Eight of twelve cavities in the STF-2 cryomodules achieved above 31.5 MV/m as the ILC specification.

After the second cool-down test, the RF system was drastically changed, that is, the change from 5 MW klystron to 10 MW (multi-beam) klystron including the modulator, and the single waveguide system for the single cavity to multi-waveguide system for eight cavities as shown in Figure 1. And, the LLRF control system was also changed.

The third cool-down test in late 2016 was done with the capture cryomodule. At this time, fourteen 9-cell cavities were cooled down in 2K. The main purpose in the third cool-down test was to do the vector-sum operation with eight cavities, including the feedforward system, at the average accelerating gradient of 31.5 MV/m. The others are the measurement for Lorentz Force Detuning (LFD), the heat load measurement, and the Low Level RF (LLRF) study [7], and so on.

† yasuchika.yamamoto@kek.jp

Table 1: History of the STF-2 Project

Date	Content
2011~2013	V.T. for 12 cavities / RF conditioning for 12 couplers
Jul/2013~Apr/2014	Cavity string assembly
Oct/2013~Jun/2014	Cryomodule assembly
Jul/2014	Certification for high pressure gas regulation
Oct/2014~Dec/2014	1st cool-down test
Apr/2015~Jul/2015	5 MW klystron prepared
Oct/2015~Dec/2015	2nd cool-down test
Jan/2016~Jul/2016	10 MW klystron prepared
Sep/2016~Nov/2016	3rd cool-down test

CAVITY PERFORMANCE AND RADIATION LEVEL

After the cool-down, the achievable accelerating gradient for each cavity was checked again including the radiation level. Regardless of the comparable radiation level as the 2nd cool-down test, almost all cavities had the performance degradation again. Moreover, two cavities in the capture cryomodule also had the degradation, although the beamline has been kept under vacuum since 2013. The left figure in Fig. 2 shows the summary of the achievable accelerating gradient for every cavity in the capture and STF-2 cryomodules. CAV#5, #6, #7, and #9 in the STF-2 cryomodules were not tested in the 3rd cool-down test. The right figure in Fig. 2 shows the correlation plot of achievable accelerating gradient for ten cavities measured in the previous and present cool-down tests. It is clear that almost every cavity had degradation again in the 3rd cool-down test. The causes for the "more" degraded cavities are the followings:

- Change of RF system from single to multi cavity
- Not-optimized forward power to power couplers
- Earthquake

The change of RF system means that klystron, modulator, waveguide, circulator, and LLRF changed from the single cavity to multi cavity operation. Generally, there is the systematic error between the different RF systems. The change of RF system in the 3rd cool-down test may generate the change of the cavity performance.

As for the second item, during the vector-sum operation, it is necessary to keep the optimum forward power to each power coupler; however, actually, too-much forward

ISBN: 978-3-95450-191-5 doi:10.18429/JACoW-SRF2017-THYA02

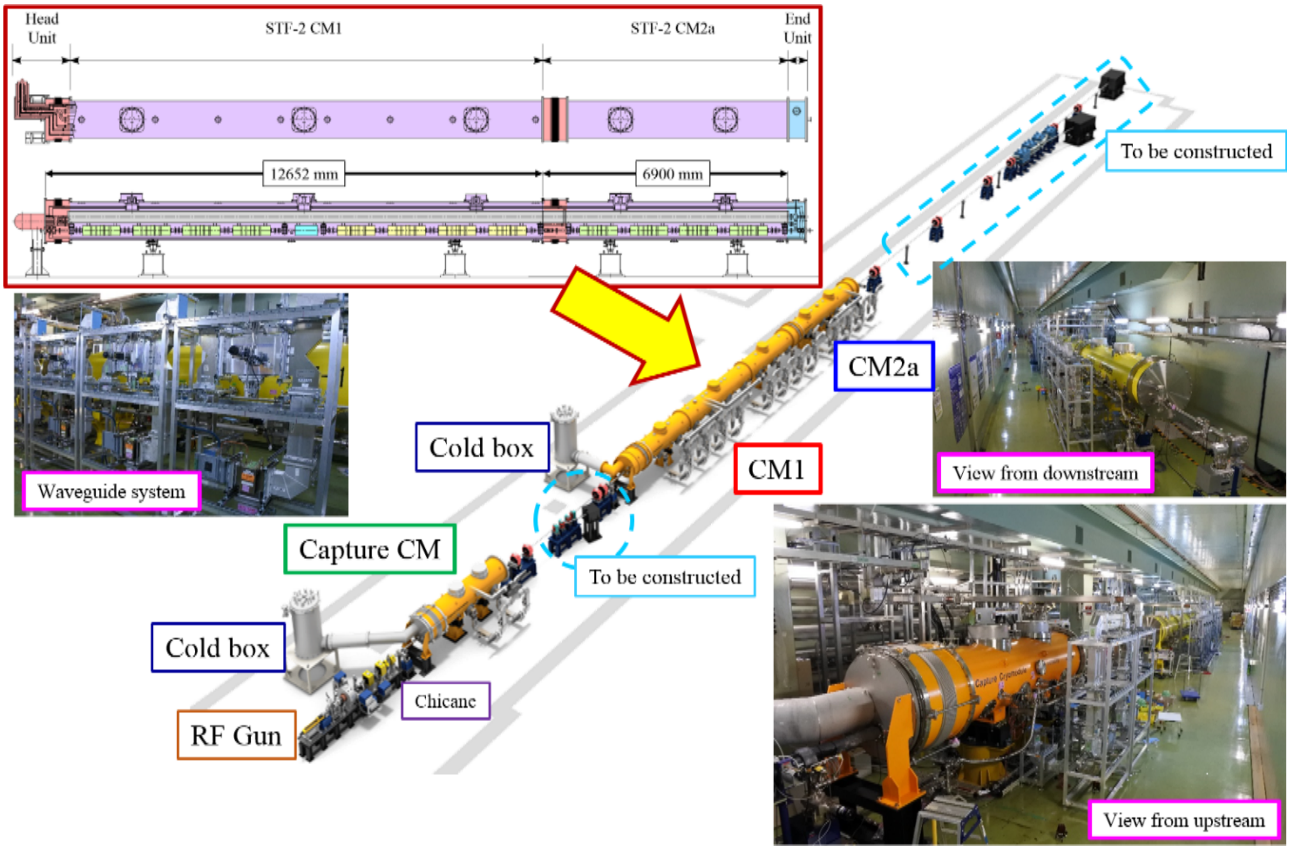

Figure 1: STF-2 Cryomodule and accelerator. The RF Gun and capture cryomodule were constructed and operated in 2012. The waveguide system is connected to two cavities in the capture cryomodule and eight cavities in the STF-2 cryomodule. The beamlines in the upstream and downstream of the STF-2 cryomodule are not constructed yet.

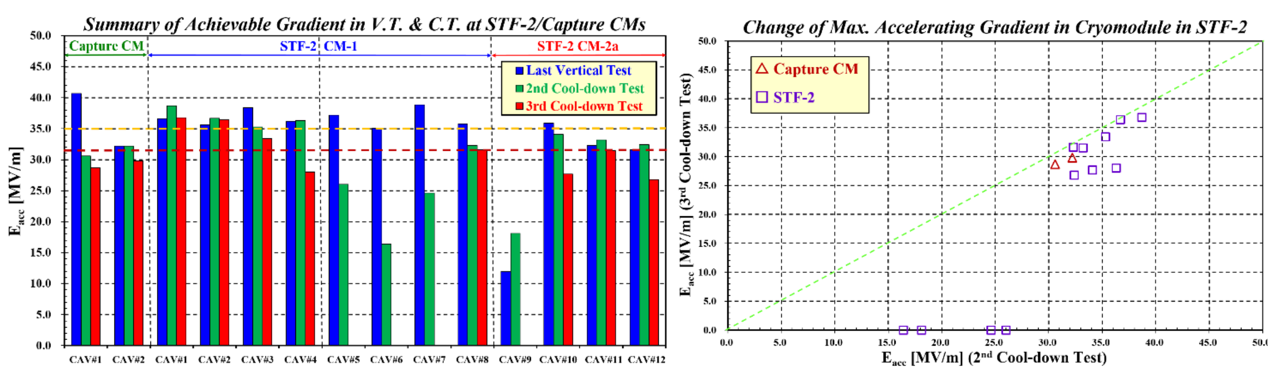

Figure 2: Summary of achievable accelerating gradient for every cavity in the capture and STF-2 cryomodules (left), and the correlation plot of achievable accelerating gradient between 2nd and 3rd cool-down test (right). Four cavities on the horizontal axis were not measured in the 3rd cool-down test.

power has been delivered. This effect may generate the unusual vacuum burst and the "re-degradation" of the cavity performance, as which phenomenon was observed in the S1-Global cryomodule [8].

In Tsukuba-city, there are a lot of earthquakes of Level 3 and 4, which is medium level in Japan. In E-XFEL, there was no clear observation in performance degradation by the vibration effect during the cavity/cryomodule transportation [9]. However, it seems that the effect by the earthquake is not same as that by the transportation. It is necessary to keep monitoring the cavity performance more carefully in future.

During the high power test for the STF-2 cryomodule, the emitted x-rays are measured at the both of the upstream and downstream beamlines, and below each measuring cavity. The top figure in Fig. 3 shows the onset gradient measured in the last vertical test (V.T.), 2nd and 3rd cool-down tests. In the 3rd cool-down test, the onset gradient is comparable or rather higher than 2nd test. The center and bottom figures show the comparison of the radiation level in the last V.T. and two cryomodule tests for Cavity #1 and #12. There was little difference in the radiation level between two cool-down tests. From these results, it is clear

ISBN: 978-3-95450-191-5 doi:10.18429/JACoW-SRF2017-THYA02

that the field emission was not related to the "more" performance degradation in the 3rd cool-down test. This means that the unknown factor exists for the re-degradation.

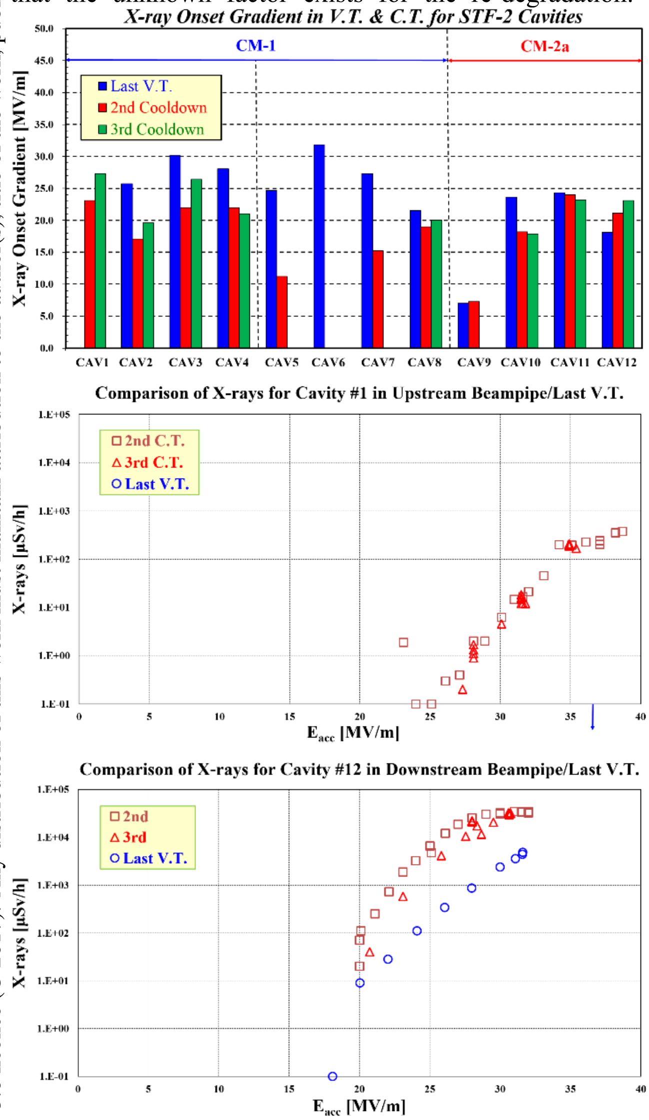

Figure 3: Comparison of x-ray onset gradient in the STF-2 cavities (top), and radiation level for Cavity #1 (center), and Cavity #12 (bottom).

LORENTZ DETUNING MEASUREMENT

The Lorentz detuning measurement was done by the pulse-shortening method during the closed-loop RF operation to keep the stable accelerating gradient in the flat-top region of RF pulse, as shown in Fig. 4. The detuning frequency at "zero" gradient is estimated by the extrapolation in the fitting curve for the "rise-up" region. This behaviour of LFD is well understood by the "two modes model" [10]. As a good trend, it is noted that the effect of LFD for the STF-2 cavities is almost same for every region. As one feature of the STF-type cavity, it has more stiffness by the thicker titanium endplate than the TESLA cavity [11]. In the higher gradient operation above 31.5 MV/m, the detuning frequency by the Lorentz force becomes much smaller, and therefore, it is more easily to do the cavity operation by the LLRF control in such higher gradient. Figure 5 shows the result of LFD for every cavity from the S1-Global to the STF-2 cryomodules. Although there is little difference in the rise-up region, the STF-type cavity has more stiffness than the TESLA cavity in the flat-top region.

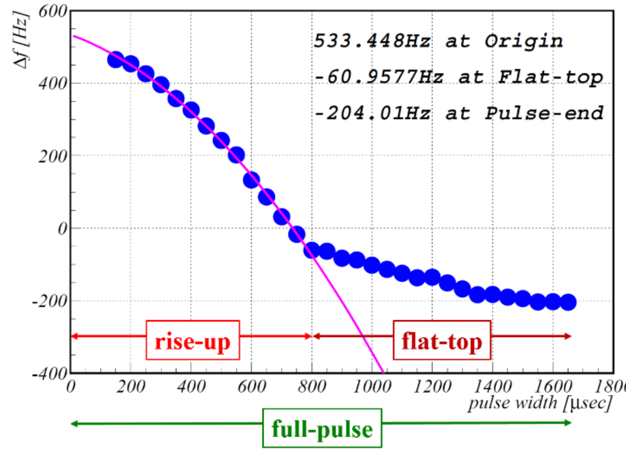

Figure 4: Example of measurement for LFD by the pulse shortening method. The purple curve is the fitting curve for all the data in the "rise-up" region.

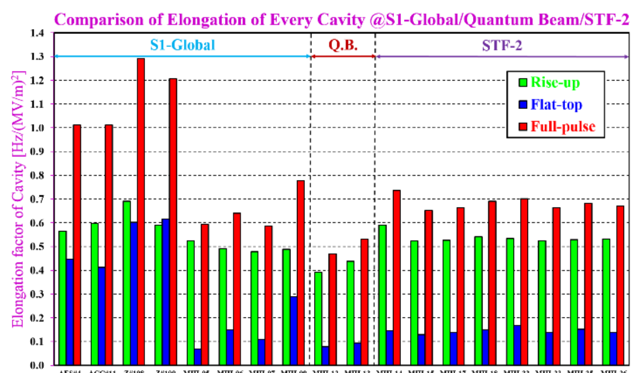

Figure 5: Comparison of the LFD for the S1-Global (w/ four TESLA cavities), the capture (named the Quantum Beam cryomodule at that time), and the STF-2 cryomodules.

HEAT LOAD MEASUREMENT

The static/dynamic heat load was estimated from the helium mass flow, measured at the downstream of helium gas return line. At this time, the static heat load of the STF-2 cryomodules including the quadrupole magnet system was 23W. In the next time, the static heat load will be measured by disconnecting the current leads to exclude the effect of the system. On the other hand, the dynamic heat load was estimated by the single cavity operation; the waveguide system is connected to only one cavity, and no other connected cavities. As the temperature sensor attached around the cavity, "DT-670C-SD", one kind of silicon diode, was used [12]. Figure 6 shows the comparison of Q-E_{acc} curve and radiation level between the vertical and cryomdoule tests for eight cavities measured in the 3rd cool-down test. The systematic error for the unloaded Q in the cryomodule test was estimated from the reproducibility of static heat

ISBN: 978-3-95450-191-5 doi:10.18429/JACoW-SRF2017-THYA02

load measurement, which was done 28 times, and the root mean square of helium mass flow distribution. The systematic error in the static heat load was 0.36 W, and the root mean square of helium mass flow was 3.9%. The RF duty was estimated to be 0.85%. The unloaded Q for every cavity in the cryomodule test was uniformly lowered than the vertical test, not related to the radiation level. This situation is same as already described in the previous section; although the radiation level was never changed in the 3rd cool-down test, the cavity performance was degraded by the unknown factor. Recently, in FNAL, it was clear that the cool-down rate of cryomodule generates to the change of unloaded Q [13]. Then, in the 4th cool-down test for the STF-2 cryomodule, the cool-down rate will be faster for the higher unloaded Q, and also the RF conditioning will be done by the shorter pulse width.

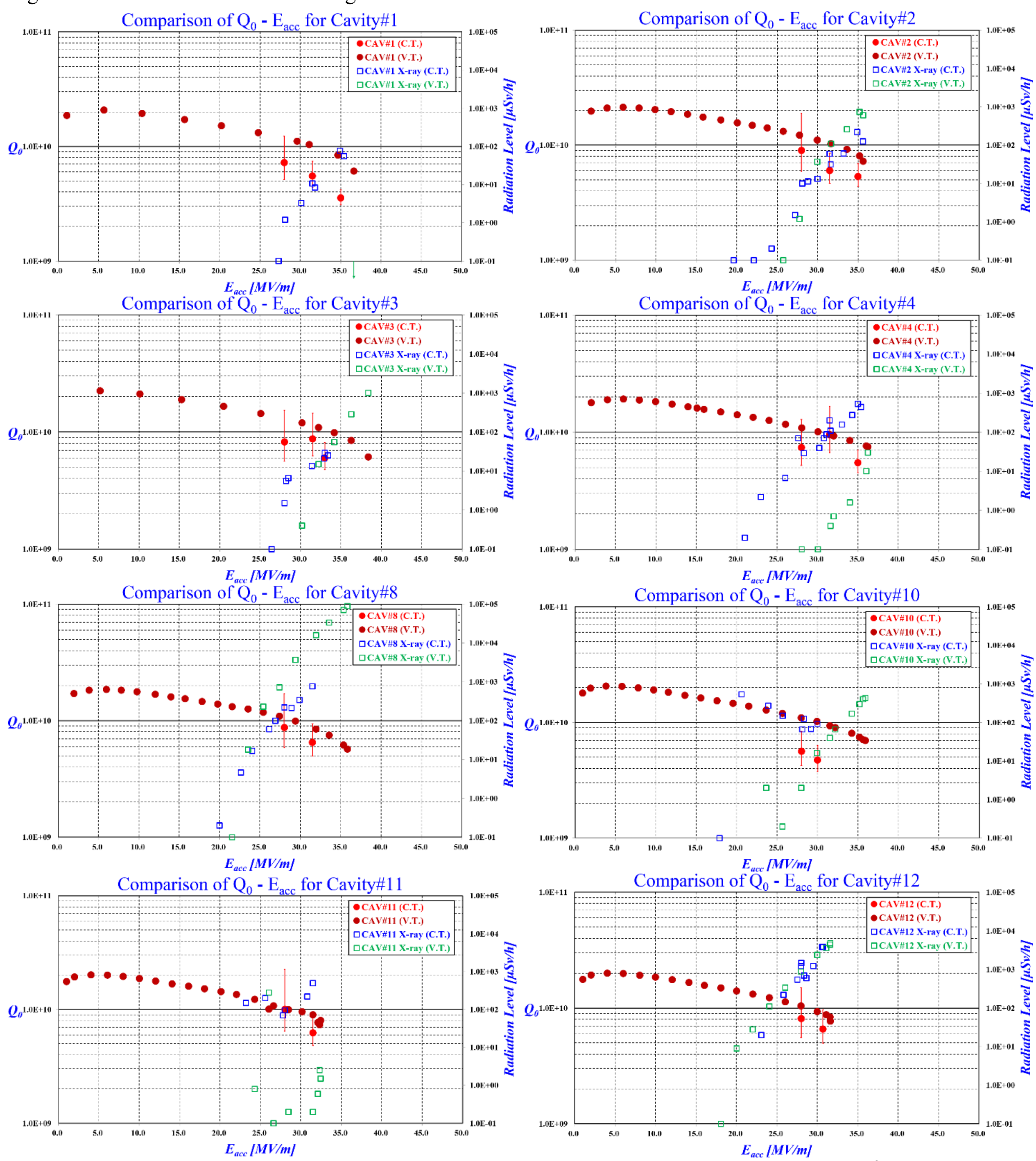

Figure 6: Comparison of the Q-E_{acc} curves and the radiation level between the last V.T. and the 3rd cool-down test for eight cavities. All Q_0 points measured in the 3rd cool-down test, which have the larger systematic errors, are lower than the last V.T. Especially, although Cavity #12 has the heavy field emission, it has the higher Q_0 points than Cavity #1.

ISBN: 978-3-95450-191-5 doi:10.18429/JACoW-SRF2017-THYA02

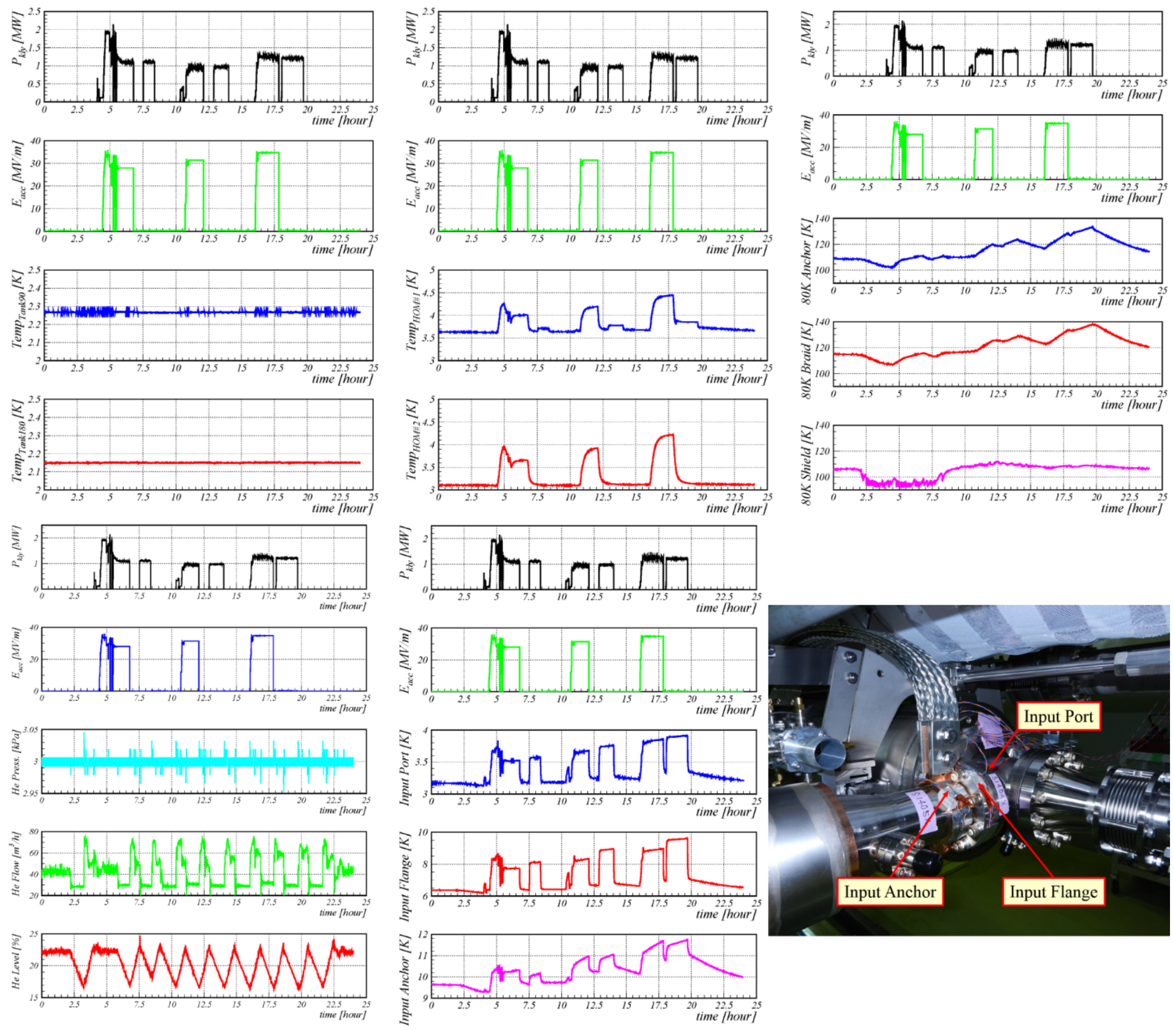

Figure 7: Daily status of temperature trend and cryogenics system during the heat load measurement for Cavity #1. In all trend graphs, the black line shows the klystron output power, and the green one shows the accelerating gradient. In the top three graphs and the bottom-centre graph, the other colour lines show the temperature at each position. "$\mathrm{Temp}_{\mathrm{Tank90,\ 180}}$" means the temperature for two different positions on the helium tank of Cavity #1. Around the port of power coupler, three sensors are attached, "Input Port", "Input Flange", and "Input Anchor", as shown in the bottom-right figure. In the bottom-left graph, the cryogenic status is shown, the light blue; the helium pressure, the green; helium mass flow, the red; the helium level measured at the downstream of the STF-2 cryomodule. During the heat load measurement, the helium pressure was stable within the fluctuation of 1%. It is mentioned that the temperature increase at the two HOM couplers, and the power coupler port was not saturated during the heat load measurement.

Figure 7 shows the daily status of the forward power, the accelerating gradient, each temperature, and the cryogenic system during the heat load measurement for Cavity #1. The helium flow was stopped to make the stable condition during the heat load measurement. Two silicon diodes were attached on the helium tank to monitor the cavity temperature. The monitoring positions around the port of the power coupler are shown in the bottom-right figure. After the RF switching off, the temperature around the power coupler, and HOM couplers was not promptly steady. This phenomenon might affect the next heat load measurement with some errors.

VECTOR-SUM OPERATION

The vector-sum operation with eight cavities was done at the average accelerating gradient of 31 MV/m by the feedback and the feedforward RF system. The piezo actuator worked for the compensation of LFD. The left figure in Fig. 8 shows the status of the vector-sum operation with eight cavities at 31 MV/m. The accelerating gradient for each cavity is shown in red. Two of eight cavities, Cavity #1 and #2, achieved around 36 MV/m, and on the other hand, three of eight cavities, Cavity #4, #10, and #12, had more significant degradation in the 3rd cool-down test, as

ISBN: 978-3-95450-191-5 doi:10.18429/JACoW-SRF2017-THYA02

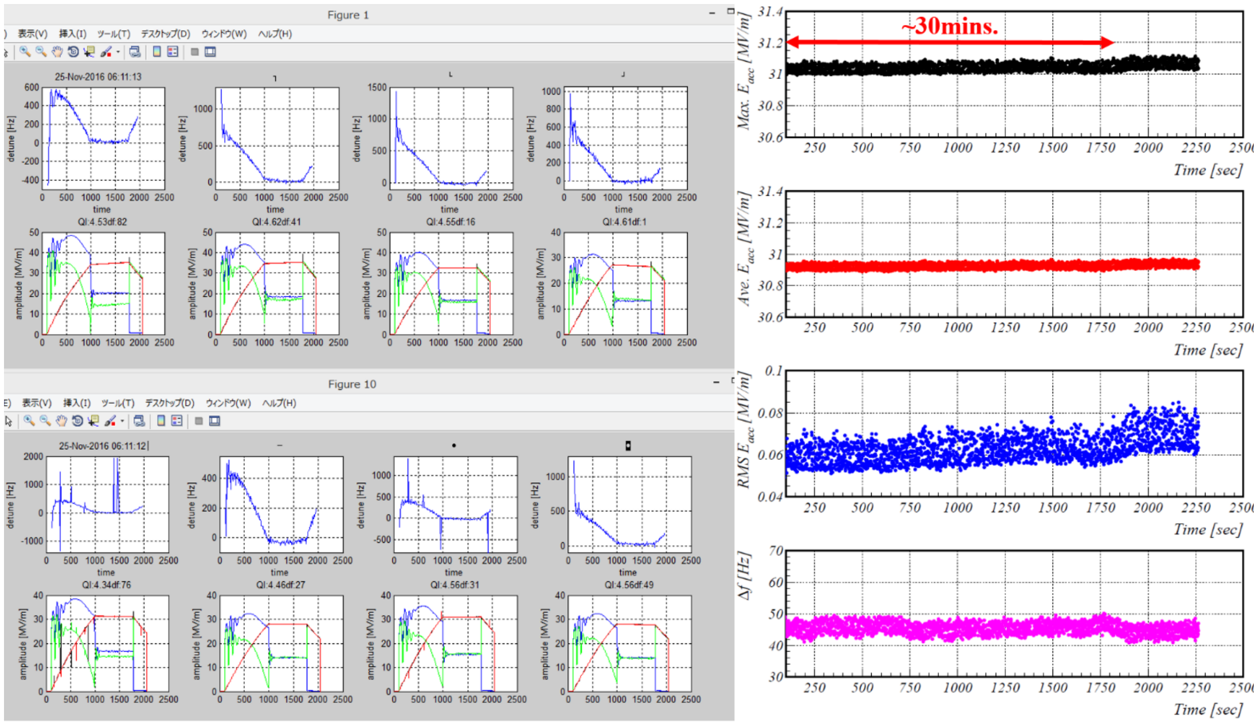

Figure 8: Left; Status of vector-sum operation with eight cavities in the STF-2 cryomodule (there are some noisy channels). The detuning frequency (blue), accelerating gradient (red), forward power (blue), and reflect power (green) are shown. Right; Trend graph for 8 cavities operation at 31 MV/m for half an hour. The Max. E_{acc} (black), the average E_{acc} (red), the root mean square of E_{acc} for the flat-top region of each pulse (blue), and the detuning frequency (purple). The stability in the average accelerating gradient and the detuning frequency is evaluated by making the histograms for these data as shown in Fig. 9.

previously described. However, the LLRF control system perfectly worked to keep the stable operation at 31 MV/m for half an hour as shown in the right figure.

Figure 9 shows the distribution of the average accelerating gradient and the detuning frequency for eight cavities during the vector-sum operation for half an hour. From these histograms, it is clear that the fluctuation in the accelerating gradient is 0.02 MV/m, and that in the detuning frequency is 1.8Hz. This means that the STF-2 cryomodules were stably operated at the ILC specification, and it is an extremely important milestone for the realization of ILC. Additionally, in this operation, the auto-feedback system was not used for the slide-jack and piezo tuners. That is the main subject for the long term operation in future.

CONCLUSION

The STF-2 cryomodules have experienced the cool-down tests three times since 2014. In the third cool-down test, the vector-sum operation with eight cavities was successfully done at 31 MV/m, as the extremely important milestone for ILC. As for the lower unloaded Q than the vertical test, the cool-down rate of the STF-2 cryomodule will be faster for the higher unloaded Q in the next cool-down test. In addition, for “more” degraded cavities, the RF conditioning by the shorter pulse width will be done in the next cryomodule test again. At present, the achievements in the STF-2 project are summarized in Table 2.

FUTURE PLAN

At present, the STF-2 cryomodule is put along the beamline in the STF tunnel. In F.Y. 2018, the fourth cool-down test will be done for some tests as described before, and the beamline construction including the beam-dump will start. The beam commissioning using the STF-2 cryomodule by the ILC specification is another important milestone as the operational demonstration of the prototype ILC accelerator.

ACKNOWLEDGEMENTS

Special thanks are given to Y. Kondo (KEK) for the temperature monitoring system; T. Yanagimachi, S. Imada, H. Yamada, and M. Asano (NAT) for the experiment preparation, operation and recording for the STF-2 cryomodules; N. Hanaka, K. Ishimoto, and N. Numata (NAT) for the LLRF/HLRF control system; A. Hayakawa (KIS) for the maintenance of control and monitoring system for the STF-2 cryomodule operation; and the HITACHI Cryogenics group for the control and maintenance for the STF cryogenic system.

ISBN: 978-3-95450-191-5 doi:10.18429/JACoW-SRF2017-THYA02

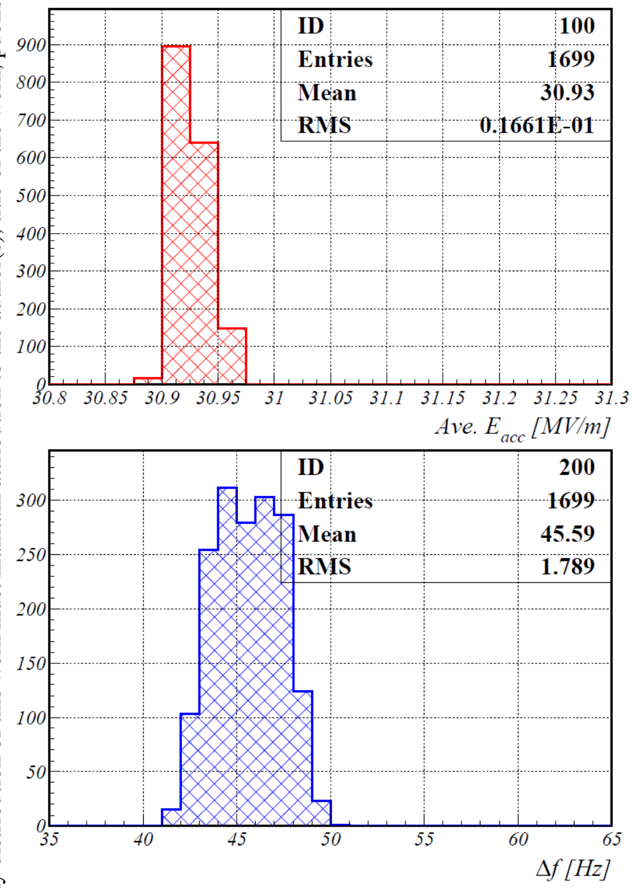

Figure 9: Stability of the average E_{acc} and the detuning frequency in the vector-sum operation with eight cavities for half an hour.

Table 2: Achievement in the STF-2 Project

Content	Achievement
Cavity performance in V.T.	9 of 12 cavities achieved above 35 MV/m
Cavity performance in C.T.	8 of 12 cavities achieved above 31.5 MV/m
Slide-jack tuner	Good performance
Piezo tuner	Good performance
Cavity stiffness	Uniform
LFD	Perfectly compensated
Heat load	Uniformly lower Q_0
Vector-sum operation	Done at 31 MV/m with 8 cavities

REFERENCES

[1] ILC Technical Design Report (2013), https://www.linearcollider.org/ILC/Publications/Technical-Design-Report

[2] V. Kashikhin *et al.*, "Compact Superconducting Magnet for Linear Accelerators", FERMILAB CONF 14 273.

[3] A. Heo *et al.*, "Status of Cold Cavity Beam Position Monitor for STF", in *Proc. IPAC'11*, pp. 1236-1238, San Sebastian, Spain.

[4] T. Shishido *et al.*, "Assembly and Cool-Down Tests of STF2 Cryomodule at KEK", in *Proc. SRF'15*, pp. 888-892, Whistler, BC, Canada.

[5] Y. Yamamoto *et al.*, "High Gradient Cavity Performance in STF-2 Cryomodule for the ILC at KEK", in *Proc IPAC'16*, pp. 2158-2160, Busan, Korea.

[6] Y. Yamamoto *et al.*, "STF-2 Cryomodule Performance and New Input Coupler R&D for ILC", in *Proc. ICHEP'16*, PoS(ICHEP2016)066, Chicago, U.S.

[7] S.B. Wibowo *et al.*, "Evaluation of Digital LLRF System Performance at STF in KEK", in *Proc. IPAC'17*, pp. 3992-3995, Copenhagen, Denmark.

[8] Y. Yamamoto *et al.*, "Cavity Degradation Experience at S1-Global", in *Proc. TTC'11*, IHEP, Beijing, China.

[9] D. Kostin, private communication, Feb. 2016.

[10] Y. Yamamoto *et al.*, "Observation and numerical calculation of Lorentz-detuning for the cryomodule test of STF baseline cavities at KEK-STF", in *Proc. PAC'09*, pp. 999-1001, Vancouver, BC, Canada.

[11] Y. Yamamoto *et al.*, "Test Results of the International S1-Global Cryomodule", in *Proc.SRF'11*, pp. 615- 624, Chicago, IL, U.S.

[12] http://www.lakeshore.com/products/cryogenic-temperature-sensors/silicon-diodes/dt-670/pages/Ordering.aspx

[13] G. Wu *et al.*, "First Results of LCLS-II Cryomodule, Q_0 Studies as Function of Cooldown", TTC Meeting 2017, M.S.U., MI, U.S.